Physically-Realizable Uniform Temperature Boundary Condition Specification on a Wall of an Enclosure: Part II – Problem Solution

P. Y. C. Lee
Kutztown University of Pennsylvania

W. H. Leong
Ryerson University

Physically-Realizable Uniform Temperature Boundary Condition Specification on a Wall of an Enclosure: Part II – Problem Solution

P.Y.C. Lee[1] and W.H. Leong[2]

[1]Department of Mathematics
Kutztown University of Pennsylvania
P.O. Box 730
Kutztown, Pennsylvania 19530
plee@kutztown.edu

[2]Department of Mechanical and Industrial Engineering
Ryerson University
350 Victoria St.
Toronto, Ontario, Canada M5B 2K3
weyleong@ryerson.ca

Abstract

Temperature measurements along one side of the rectangular plate showed severe temperature non-uniformity along one side of a wall of a cubical experimental apparatus where the uniform temperature was physically desired. Despite proper planning and analyses, this non-uniformity was high enough that a benchmark study could not be carried out to the desired accuracy of about one percent error. This paper presents and extends analyses made previously based on the modifications to the original design of the apparatus to reduce the temperature non-uniformity on the wall by adding an auxiliary heater around a wall where the uniform temperature was desired. A detailed mathematical analysis shows significant reduction in temperature non-uniformity from about four percent (based on the initial design) to less than one percent (for the modified design). By examining the temperature difference between two locations on the plate, the predicted temperature difference obtained through mathematical analyses show excellent agreement with the measured temperature difference. The temperature non-uniformity along the boundary of a wall was reduced to less than one percent of the overall temperature difference.

55

1. Introduction

Computational fluid dynamics (CFD) has played a very important role in the heat transfer industry by enhancing performance to existing designs or by developing new designs for better performance, and by diagnosing issues related to existing designs and finding solutions to these issues. Example where CFD is used is in the design of effective cooling of the moderator fluid in a nuclear reactor where heat removal is paramount so that over-heating of nuclear fuel channels does not occur (He and Gotts (2005) and Lee and Collins (1998)). Ultimately, to a designer and/or an analyst, a "good" CFD code is one that can model a myriad of heat transfer engineering problems with a high degree of confidence.

For numerical modelers, it is important to test their model against available and accurate experimental data based on a well-defined "simple" problem. Depending on the type of problem considered to test their model, there may be no experimental data that can validate their model. Benchmark problems have been investigated by de Vahl Davis (1983) and de Vahl Davis and Jones (1983) to compare numerical results between different CFD codes for simple boundary conditions but there is little research work in comparing numerical results with experimental results. For example, two-dimensional and three-dimensional benchmark problems in internal natural convection heat transfer assume an adiabatic wall or a uniform temperature along a wall or a combination of both of these conditions. Although the adiabatic boundary condition has been solved for various numerical problems, the actual implementation of this case for an experimental study is not physically realistic (La Quere (1991)). For adiabatic wall cases, to validate a numerical solution against experimental data with high degree of accuracy is remote as adiabatic cases are physically difficult to achieve (El Sherbiny et al. (1982)). For internal natural convection problems which involve a uniform temperature boundary condition, very few research work have been conducted where numerical solutions are compared with experimental data (for example, Leong et al. (1998) and (1999)).

This paper will demonstrate that a physically-realizable "uniform" boundary condition imposed on a three-dimensional experimental apparatus for benchmark natural convection study can be achieved with a proper design (Leong et al. (1998) and (1999), and Leong (1996)). The study involves measuring accurate Nusselt numbers, Nu, to be around 1% error for a wide range of Rayleigh numbers Ra. The experimental set-up is discussed in detail by Leong (1996), and a summary of the cubical experimental apparatus can be found by Lee and Leong (2013), but it is also summarized here.

The experimental apparatus is represented in Figure 1 with the thermal boundary conditions imposed on the walls of the cubical enclosure, which is made up of two opposing main plates/walls and four sidewalls. The temperatures of the two main plates are designed to be constant across each of the entire face (where one plate is at a "hot" temperature T_h while the other opposing plate is at a "cold" temperature T_c). The temperatures on the four remaining walls (called the *sidewalls*) all vary linearly between the two main walls, as shown in Figure 1.

C. Lee and Leong: Temperature Boundary Condition on a Wall of an Enclosure: Part II

AAM: Intern. J., Vol. 8, Issue 1 (June 2013)   57

$$T = T_h - (T_h - T_c)\, x/L$$


$$T = T_h - (T_h - T_c)\, x/L$$
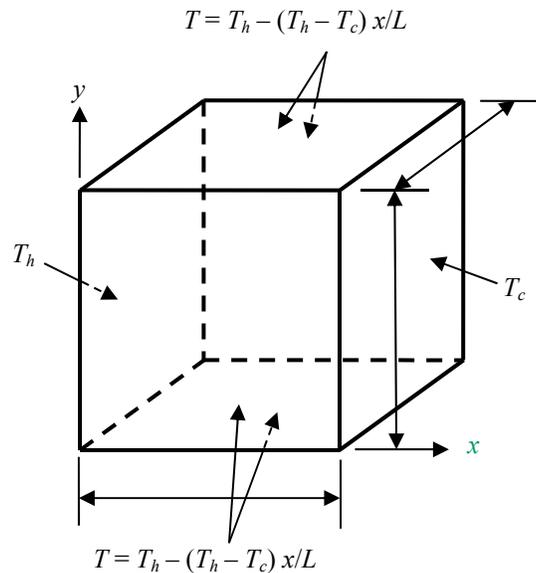
Figure 1. Idealized cubical enclosure with its thermal boundary conditions

As indicated by Leong (1996) and Lee and Leong (2013), temperature difference measurements made between two points in the "hot" plate along the bottom-interior surface was in the excess of 4% of ΔT (= $T_h - T_c$). It was apparent from this difference that temperature non-uniformity existed on the "hot" plate. Although this temperature non-uniformity is small, this was large enough to render the benchmark study of internal natural convection heat transfer unattainable to the desired Nusselt number accuracy of about 1%. In supporting these measurements, a detailed mathematical analysis was performed to investigate this temperature non-uniformity on the "hot" plate, and it was determined that this temperature non-uniformity was a result of the effect of thermal spreading/constriction resistance (Leong (1996) and Lee and Leong (2013)). A thermal resistance model was developed using an approximate analytical temperature solution based on a boundary value problem of the "hot" plate. As a result, design changes had to be made to the apparatus to reduce the temperature non-uniformity to an acceptable level (to less than 1%) between the contact region and the entire "hot" plate, so that a "uniform" temperature boundary condition can be deemed appropriate for the experimental natural convection benchmark study.

Due to time and budget constraints, redesigning the entire apparatus would not have been feasible (Leong (1996)). The decision was to use the existing apparatus, and add auxiliary heaters along the "exterior" portions of the "hot" plate (see Figures. 2 and 3a). The addition of heat from the exterior regions of the plate would enable heat to flow to the sidewalls and the plate, thereby reducing the temperature non-uniformity in the interior side of the "hot" plate (see Figure 3a). In order to understand the effect of the additional heat supplied by the auxiliary heaters to the "hot" plate, a detailed analysis was required, and to assess whether a reduction of the temperature non-uniformity in the interior side of hot plate to less than 1% of ΔT is indeed attainable.
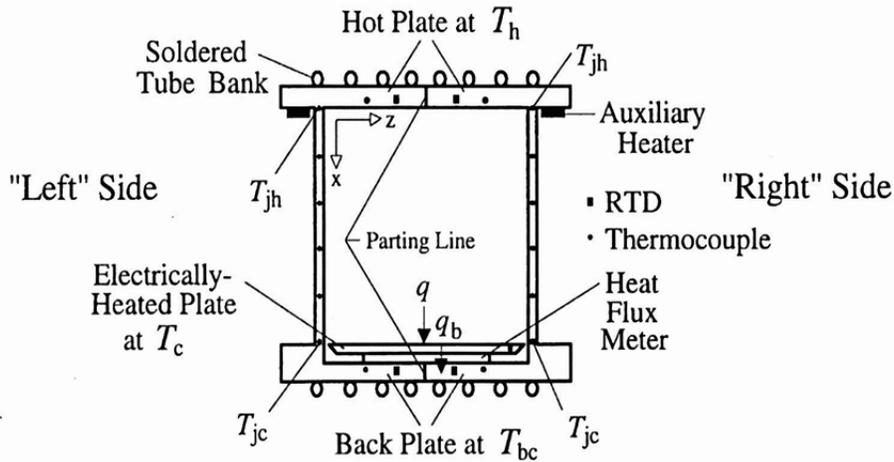
Figure 2. Cubical experimental apparatus with auxiliary heaters
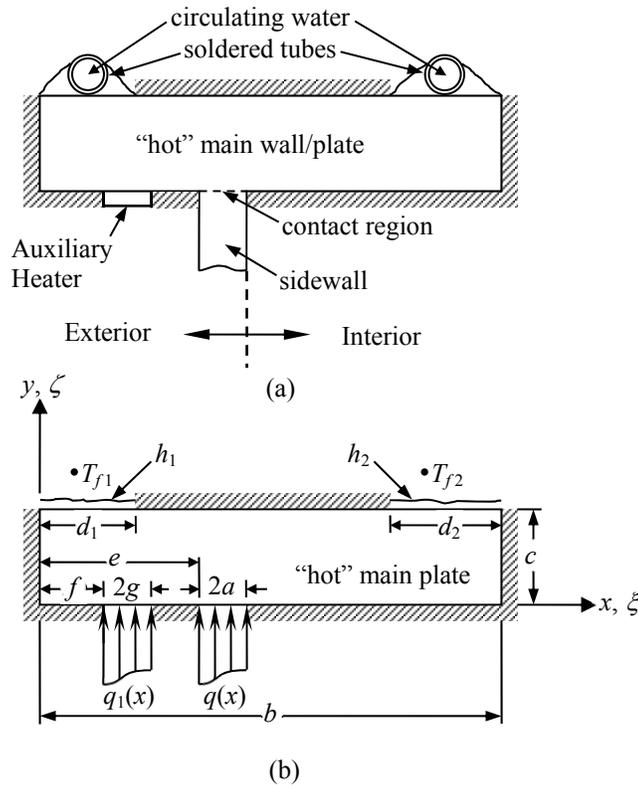
Figure 3. (a) A simplified sketch of the physical problem
(b) Boundary value problem with boundary conditions and
defined parameters

In this paper, an extension to an approximate analytical solution to the one presented by Lee and Leong (2013) is presented, which incorporates the heat flux boundary conditions (or inhomogeneous Robin boundary conditions) due to the auxiliary heaters. Comparisons of the approximate analytical temperature solution with a numerically converged finite-element

C. Lee and Leong: Temperature Boundary Condition on a Wall of an Enclosure: Part II

AAM: Intern. J., Vol. 8, Issue 1 (June 2013) 59

solution have shown excellent agreement over practical range of interest (Lee and Leong (2013)). Based on this extended/generalized solution, a detailed mathematical analysis is conducted, and a rationale for positioning the auxiliary heaters in the "exterior" portion of the "hot" plate will be presented. In the process, a thermal resistance analysis will be developed and applied to validate the approximate analytical results with measured data (Leong (1996)).

2. Problem Description

Mathematical Statement of the Problem

The physical layout of the present problem is similar to the one defined by Lee and Leong (2013), but incorporates the presence of the auxiliary heaters in the exterior portions of the "hot" plate as shown in Figs. 3a and 3b. The width and the thickness of the plate are denoted by b and c, respectively. The *contact* region where the sidewall meets the "hot" plate is modeled as a heat flux source/sink with a prescribed distribution $q(x)$ over a contact length of $2a$ at a distance e from the y-axis. The auxiliary heater is positioned f (which must be less than or equal to $e - 2g$) away from the y-axis, and its heat flux $q_1(x)$ is prescribed with a contact length of $2g$. On the opposite side of the "hot" plate, two sub-sections have been modeled to represent a set of tube banks which is in contact with two different circulating fluid temperatures at T_{f1} and T_{f2} with contact widths d_1 and d_2, and with convective heat-transfer coefficients h_1 and h_2, respectively. The remaining surfaces are assumed adiabatic. All other assumptions used in the analysis are provided by Lee and Leong (2013).

The differential equation to be solved is Laplace's equation in temperature T. It is assumed that there are no transient effects (that is, steady-state heat conduction only), and the material of the plate is a homogeneous, isotropic conductor with thermal conductivity k, and with no internal heat generation:

$$\frac{\partial^2 T}{\partial x^2} + \frac{\partial^2 T}{\partial y^2} = 0, \tag{1}$$

with the boundary conditions specified along all four sides given by:

$$x = \mathbf{0}, 0 \le y \le c: \quad \frac{\partial T}{\partial x} = 0, \tag{2a}$$

$$x = \mathbf{b}, 0 \le y \le c: \quad \frac{\partial T}{\partial x} = 0, \tag{2b}$$

$$y = \mathbf{0}, 0 \le x \le f: \quad \frac{\partial T}{\partial y} = 0,$$

$$f \le x \le f + 2g: \quad \frac{\partial T}{\partial y} = \frac{-q_1(x)}{k}, \quad f + 2g \le x \le e: \quad \frac{\partial T}{\partial y} = 0,$$

$$e \le x \le e + 2a: \quad \frac{\partial T}{\partial y} = \frac{-q(x)}{k}, \quad e + 2a \le x \le b: \quad \frac{\partial T}{\partial y} = 0, \tag{2c}$$

$$y = c, \; 0 \le x \le d_1: \; \frac{\partial T}{\partial y} = -\frac{1}{k} h_1 \big[T(x,c) - T_{f1}\big],$$

$$d_1 \le x \le b - d_2: \; \frac{\partial T}{\partial y} = 0, \; b - d_2 \le x \le b: \; \frac{\partial T}{\partial y} = -\frac{1}{k} h_2 \big[T(x,c) - T_{f2}\big]. \qquad (2d)$$

3. Analytical Solution

Dimensionless variables similar to those defined by Lee and Leong (2013) are introduced:

$$\xi \equiv \frac{x}{b}, \qquad \zeta \equiv \frac{y}{b}, \qquad T^* \equiv \frac{kL(T - \overline{T_f})}{Q}, \qquad (3)$$

where

$$\overline{T_f} = \frac{d_1 h_1 T_{f1} + d_2 h_2 T_{f2}}{d_1 h_1 + d_2 h_2} \qquad (4)$$

is the weighted-average of the fluid temperature, and

$$Q = L \int_e^{e+2a} q(x) \, dx \qquad (5)$$

is the total heat flow at the *sidewall* (or contact) due to $q(x)$ over length L (into the page). Additional dimensionless parameters are introduced:

$$\varepsilon \equiv \frac{a}{b}, \delta \equiv \frac{f}{b}, \alpha \equiv \frac{c}{b}, \beta_1 \equiv \frac{d_1}{b}, \beta_2 \equiv \frac{d_2}{b}, \eta \equiv \frac{e}{b}, \rho \equiv \frac{g}{b}, \qquad (6)$$

and from Equation (3), the dimensionless fluid temperatures are given by

$$T_{f1}^* = \frac{kL\big(T_{f1} - \overline{T_f}\big)}{Q}, \qquad T_{f2}^* = \frac{kL\big(T_{f2} - \overline{T_f}\big)}{Q}, \qquad (7)$$

where the average fluid temperature (Equation (4)) expressed in terms of dimensionless variables is

$$\overline{T_f} = \frac{\beta_1 Bi_1 T_{f1} + \beta_2 Bi_2 T_{f2}}{\beta_1 Bi_1 + \beta_2 Bi_2}, \qquad (8)$$

and the Biot numbers/moduli, *Bi*, are defined by

C. Lee and Leong: Temperature Boundary Condition on a Wall of an Enclosure: Part II

AAM: Intern. J., Vol. 8, Issue 1 (June 2013)   61

$$Bi_1 \equiv \frac{h_1 \, b}{k}, \qquad Bi_2 \equiv \frac{h_2 \, b}{k} \ . \tag{9}$$

The separation of variables method was used for finding the approximate solution to Laplace's equation, Equation (1) as used by Lee and Leong (2013). An approximate analytical solution to the temperature field, in dimensionless form, is given by:

$$T^*(\xi,\zeta) = Q^*(\gamma - \zeta)$$

$$+ \sum_{n=1}^{\infty} \left\{ \left(\phi_n \left[T_{f1}^* - Q^*(\gamma - \alpha) \right] - \chi_n \left[T_{f2}^* - Q^*(\gamma - \alpha) \right] \right) \cos(n\pi\xi) \cosh\left(n\pi\zeta \right) \right\} \tag{10}$$

$$+ \sum_{n=1}^{\infty} \left\{ \frac{2}{n\pi} H_n \cos(n\pi\xi) \left[\psi_n \cosh(n\pi\zeta) - \sinh(n\pi\zeta) \right] \right\},$$

where

$$\gamma = \alpha + \frac{1}{\beta_1 \, Bi_1 + \beta_2 \, Bi_2} \ , \tag{11a}$$

$$H_n = \frac{bL}{Q} \left(\int_{\delta}^{\delta+2\rho} q_1(\xi) \cos(n\pi\xi) \, d\xi + \int_{\eta}^{\eta+2\varepsilon} q(\xi) \cos(n\pi\xi) \, d\xi \right), \tag{11b}$$

$\varphi_n, \chi_n, \psi_n, \sigma_{i,n}$ are functions defined by Lee and Leong (2013), and

$$Q^* = 1 + \theta \ , \tag{11c}$$

where

$$\theta = \int_{\delta}^{\delta+2\rho} q_1(\xi) d\xi \Bigg/ \int_{\eta}^{\eta+2\varepsilon} q(\xi) \ d\xi . \tag{11d}$$

It is important to note here that the approximate solution given by Equation (10) is based on the assumption that the orthogonality condition of the cosine basis function (used in the infinite Fourier series solution) applies along the two subsections where the fluid is in contact with the solid. A detailed discussion of this orthogonality assumption and a comparison of the finite-element method (FEM) solution comparison with the approximate analytical solution appear in Lee and Leong (2013).

4. Analysis Approach

Thermal Resistance Network

To begin the analysis, Figure 4 illustrates a simplified network of thermal resistances based on the flow of heat due to the boundary conditions. As shown in the figure, the circulating fluid has

been "lumped" to a representative temperature T_f (as defined in Equation 4), and as well, average temperatures for the auxiliary heater and the contact at the sidewall are denoted by T_{ht} and T_c, respectively.
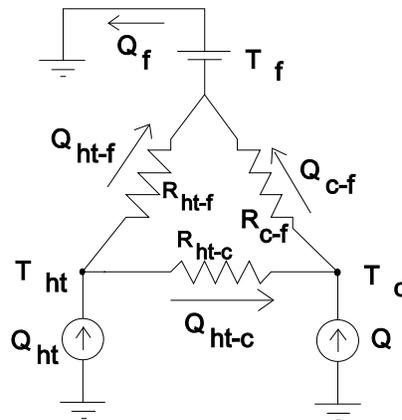

Figure 4. Simplified network of thermal resistances in the "hot" main plate

Each component of thermal resistance network is defined by the following general expression:

$$R_{1-2} \equiv \frac{\overline{T_1} - \overline{T_2}}{Q_{1-2}}, \tag{12a}$$

where R_{1-2} is the thermal resistance between the two locations 1 and 2 based on the respective mean temperatures $\overline{T_1}$ and $\overline{T_2}$ for the heat flow rate Q_{1-2} between these two locations. Also, thermal resistance, $R_{1,2}$, is defined as:

$$R_{1,2} \equiv \frac{\overline{T_1} - \overline{T_2}}{Q}. \tag{12b}$$

Note that the difference between Equations (12a) and (12b) is that Equation (12b) is the thermal resistance between two locations 1 and 2, but is based on the *heat flow imposed at the sidewall* (or *contact*), Q (which is defined in Equation (5)). For example, based on Equation (12b), the thermal resistance between the contact (sidewall) region and the circulating fluid is expressed by:

$$R_{c,f} = \frac{\overline{T_c} - \overline{T_f}}{Q}, \tag{13}$$

where

$$\overline{T_c} = \frac{1}{2a} \int_e^{e+2a} T(x,0) \, dx, \tag{14}$$

C. Lee and Leong: Temperature Boundary Condition on a Wall of an Enclosure: Part II

AAM: Intern. J., Vol. 8, Issue 1 (June 2013)   63

or

$$\overline{T}_c^{\,*} = \frac{kL(\overline{T}_c - \overline{T}_f)}{Q} = \frac{1}{2\varepsilon} \int_\eta^{\eta+2\varepsilon} T^*(\xi, 0)\, d\xi .$$ (15)

Equation (13) can be represented as dimensionless resistance defined by

$$R_{c,f}^* \equiv R_{c,f} kL = \frac{kL(\overline{T}_c - \overline{T}_f)}{Q},$$ (16)

which in turn can be expressed in terms of the average dimensionless temperature over the contact region as given by Equation (15):

$$R_{c,f}^* = \overline{T}_c^{\,*} = \frac{1}{2\varepsilon} \int_\eta^{\eta+2\varepsilon} T^*(\xi, 0)\, d\xi .$$ (17)

The purpose of the addition of Q_{ht} into the "hot" plate by the auxiliary heater is to "smoothen-out" the temperature non-uniformity in the bottom-interior surface of the "hot" plate (or to reduce the effect of thermal spreading/constriction resistance between the contact region of sidewall and the circulating fluid). Since the extent of temperature non-uniformity will also depend on the location f and the contact length $2g$ of the applied heat flux by the auxiliary heater, an "optimal" or a suitable position needs to be determined based on Q_{ht}. To achieve this task, it is desired to analyze the heat flow from the auxiliary heater to the sidewall, Q_{ht-c}, and to determine the effect of thermal resistance between the auxiliary heater and the sidewall R_{ht-c}.

From Equations (12a) and (12b), thermal resistance R_{ht-c} can be expressed as:

$$R_{ht-c} = \frac{\overline{T}_{ht} - \overline{T}_c}{Q_{ht-c}} = \frac{Q}{Q_{ht-c}} \left[\frac{\overline{T}_{ht} - \overline{T}_f}{Q} - \frac{\overline{T}_c - \overline{T}_f}{Q} \right] = \frac{Q}{Q_{ht-c}} \left(R_{ht,f} - R_{c,f} \right).$$ (18a)

In dimensionless form, the above equation can be rewritten as

$$R_{ht-c}^* \equiv R_{ht-c} k L = \frac{Q}{Q_{ht-c}} (R_{ht,f}^* - R_{c,f}^*).$$ (18b)

To obtain Q_{ht-c}, a heat balance at the contact (sidewall) junction in Figure 4 reveals that:

$$Q_{ht-c} = Q_{c-f} - Q = \frac{\overline{T}_c - \overline{T}_f}{R_{c-f}} - Q = Q\left(\frac{R_{c,f}^*}{R_{c-f}^*} - 1 \right).$$ (19a)

Equation (18b) is rewritten by using Equation (19a) to obtain:

P. Y. C. Lee and W. H. Leong

$$R_{ht-c}^* = \frac{R_{ht,f}^* - R_{c,f}^*}{\left(\dfrac{R_{c,f}^*}{R_{c-f}^*} - 1 \right)} , \tag{19b}$$

where (and it can be shown using the dimensionless thermal resistance (e.g. Equation (17)) and temperature (Equation (10)) that)

$$R_{ht,f}^* = Q^* \gamma$$

$$+ \sum_{n=1}^{\infty} \left\{ \frac{1}{n\pi\rho} \left[\phi_n \left(T_{f1}^* - Q^*(\gamma - \alpha) \right) - \chi_n \left(T_{f2}^* - Q^*(\gamma - \alpha) \right) \right] \cos(n\pi(\delta + \rho)) \sin(n\pi\delta) \right\} \tag{20a}$$

$$+ \sum_{n=1}^{\infty} \left\{ \frac{2}{n^2\pi^2\rho} H_n \psi_n \cos(n\pi(\delta + \rho)) \sin(n\pi\delta) \right\},$$

and

$$R_{c,f}^* = Q^* \gamma$$

$$+ \sum_{n=1}^{\infty} \left\{ \frac{1}{n\pi\varepsilon} \left[\phi_n \left(T_{f1}^* - Q^*(\gamma - \alpha) \right) - \chi_n \left(T_{f2}^* - Q^*(\gamma - \alpha) \right) \right] \cos(n\pi(\eta + \varepsilon)) \sin(n\pi\varepsilon) \right\} \tag{20b}$$

$$+ \sum_{n=1}^{\infty} \frac{2}{n^2\pi^2\varepsilon} H_n \psi_n \cos(n\pi(\eta + \varepsilon)) \sin(n\pi\varepsilon).$$

In Equation (19b), R_{c-f}^* is the thermal resistance between the contact region of the sidewall and the circulating fluid. For the problem without the auxiliary heater, R_{c-f}^* is equal to $R_{c,f}^*$, and can be inferred from Equation (20b), since $Q_{c-f} = Q$, $q_1(\xi) = 0$, and $Q^* = 1$ for this case as obtained by Lee and Leong (2013). As a result,

$$R_{c-f}^* = \gamma$$

$$+ \sum_{n=1}^{\infty} \left\{ \frac{1}{n\pi\varepsilon} \left[\phi_n \left(T_{f1}^* - (\gamma - \alpha) \right) - \chi_n \left(T_{f2}^* - (\gamma - \alpha) \right) \right] \cos(n\pi(\eta + \varepsilon)) \sin(n\pi\varepsilon) \right\}. \tag{21}$$

$$+ \sum_{n=1}^{\infty} \frac{2}{n^2\pi^2\varepsilon} \left[\frac{bL}{Q} \int_{\eta}^{\eta+2\varepsilon} q(\xi) \cos(n\pi\xi) \, d\xi \right] \psi_n \cos(n\pi(\eta + \varepsilon)) \sin(n\pi\varepsilon).$$

To determine how much heat flows from the auxiliary heater to the sidewall Q_{ht-c}, the ratio of heat flow into the contact region to the heat flow generated by the auxiliary heater, Q_{ht-c} / Q_{ht} is calculated. From Equation (19a), this fraction is given by

C. Lee and Leong: Temperature Boundary Condition on a Wall of an Enclosure: Part II

AAM: Intern. J., Vol. 8, Issue 1 (June 2013) 65

$$\frac{Q_{ht-c}}{Q_{ht}} = \frac{Q}{Q_{ht}}\left(\frac{R^*_{c,f}}{R^*_{c-f}} - 1\right) = \frac{1}{\theta}\left(\frac{R^*_{c,f}}{R^*_{c-f}} - 1\right),$$ (22)

where θ is given in Equation (11d).

5. Special Cases for the Heat Flux Profiles

In this section, three different heat flux profiles will be assumed initially, but the choice of one of these profiles will be discussed later. As suggested by Schneider et al. (1980) and recently adopted by Lee and Leong (2013), the heat flux profiles to be considered are given by

$$q(x) = q_0\left(1 - u^2\right)^m, \qquad m = \text{-1/2, 0, 1/2}$$ (23a)

and

$$q_1(x) = q_{01}\left(1 - v^2\right)^t, \qquad t = \text{-1/2, 0, 1/2,}$$ (23b)

where q_0 and q_{01} are constant heat flux/parameters at the sidewall (or contact) and the auxiliary heater, respectively. Local co-ordinate systems u and v are used to prescribe the heat flux distributions at the sidewall and at the auxiliary heater locations, respectively:

$$u \equiv \frac{1}{a}(x - e) - 1 = \frac{1}{\varepsilon}(\xi - \eta) - 1,$$ (24a)

and

$$v \equiv \frac{1}{g}(x - f) - 1 = \frac{1}{\rho}(\xi - \delta) - 1.$$ (24b)

These heat flux distributions, given in Equations (23), are shown graphically in Figure 5.
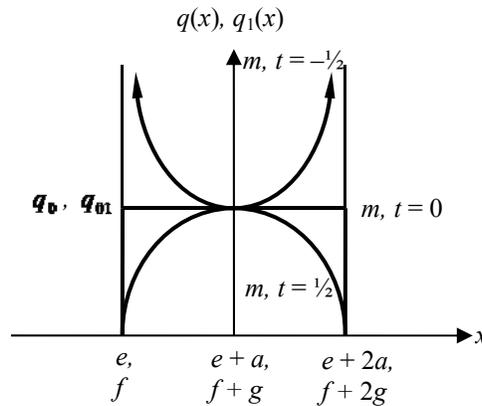
Figure 5. Three cases of heat flux profiles

Due to heat flux profiles given in Equations (23), Equation (11b), H_n, can be rewritten, as:

$$H_n = H_n(q^*, \delta, \eta) = F_n(\eta, \varepsilon) + q^* G_n(\delta, \rho), \qquad (25)$$

where

$$q^* = \frac{q_{01}}{q_0}\left(\frac{\rho}{\varepsilon}\right), \qquad (26)$$

$F_n(\eta, \varepsilon)$ is a functional form (based on the heat flux profile at the sidewall) defined by Lee and Leong (2013), and

$$G_n(\delta, \rho) = \frac{\int_{-1}^{1}(1 - v^2)^t \cos(n\pi\rho v + (n\pi(\delta + \rho)))dv}{\int_{-1}^{1}(1 - u^2)^m du}. \qquad (27)$$

It is important to note here that an additional dimensionless group q^* defined by Equation (26) has been introduced, and it depends on the parameters q_{01} and q_0, and the contact widths of the contact $2a$ and the auxiliary heater $2g$.

At the contact, it was determined that the overall thermal resistance and the thermal spreading/constriction resistance of the plate are insensitive to the choice of the heat flux profile (Lee and Leong (2013), and Schneider et al. (1980)). As a result, the uniform heat flux profile ($m = 0$) at the contact will be used for the present analysis. Therefore, the functional form $F_n(\eta, \varepsilon)$ with $m = 0$, which is given by

$$F_n(\eta, \varepsilon) = \frac{\sin(n\pi\varepsilon)\cos(n\pi(\eta + \varepsilon))}{n\pi\varepsilon}, \qquad (28)$$

will be used hereafter (Lee and Leong (2013)). The choice of the heat flux profile for the auxiliary heater will be discussed later in the next section.

Table 1 lists the functional forms of Equation (27) for $t = -1/2$, 0, and 1/2 with $m = 0$ in terms of trigonometric and Bessel functions (Gradshteyn and Ryzhik (1965)). Also, since θ (given by Equation (11d)) is a ratio of the total heat flow rate supplied by the auxiliary heater to the total heat flow rate at the sidewall, its dependence on t for $m = 0$ are also listed in Table 1.

Table 1. Functional forms of $G_n(\delta, \rho)$ and θ based on the choice of T for $m = 0$

t	$G_n(\delta, \rho)$	θ
-1/2	$\pi J_0(n\pi\rho)\cos(n\pi(\delta + \rho))$	$\pi q^* / 2$
0	$\sin(n\pi\rho)\cos(n\pi(\delta + \rho))/n\pi\rho$	q^*
1/2	$2 J_1(n\pi\rho)\cos(n\pi(\delta + \rho))/n\rho$	$\pi q^* / 4$

C. Lee and Leong: Temperature Boundary Condition on a Wall of an Enclosure: Part II

AAM: Intern. J., Vol. 8, Issue 1 (June 2013) 67

6. Results and Discussion

The general solutions provided in Equations (10), (20a), and (20b) are now used for the dimensions of the "hot" plate (Leong (1996) and Lee and Leong (2013)): $2a = 3.2$ mm, $b = 78$ mm, $c = 9.53$ mm, $d_1 = d_2 = d = 22$ mm, and $e = 11$ mm.

Using these parameters, Equations (10), (20a), and (20b) are given by

$$T^*(\xi,\zeta) = T^* = Q^*(\gamma - \zeta) + 2Q^*(\gamma - \alpha) \sum_{n=2,4,6...}^{\infty} \chi_n \cos(n\pi\xi) \cosh(n\pi\zeta)$$
$$+ \sum_{n=1}^{\infty} \frac{2}{n\pi} \cdot H_n \cdot \cos(n\pi\xi) \left[\psi_n \cosh(n\pi\zeta) - \sinh(n\pi\zeta) \right], \tag{29}$$

$$R^*_{ht,f} = Q^*\gamma + 2Q^*(\gamma - \alpha) \sum_{n=2,4,6...}^{\infty} \left\{ \frac{\chi_n}{n\pi\rho} \cos(n\pi(\delta + \rho)) \sin(n\pi\rho) \right\}$$
$$+ \sum_{n=1}^{\infty} \left\{ \frac{2}{n^2\pi^2\rho} H_n \cdot \psi_n \cdot \cos(n\pi(\delta + \rho)) \sin(n\pi\rho) \right\}, \tag{30}$$

and

$$R^*_{c,f} = Q^*\gamma + 2Q^*(\gamma - \alpha) \sum_{n=2,4,6...}^{\infty} \left\{ \frac{\chi_n}{n\pi\varepsilon} \cos(n\pi(\eta + \varepsilon)) \sin(n\pi\varepsilon) \right\}$$
$$+ \sum_{n=1}^{\infty} \left\{ \frac{2}{n^2\pi^2\varepsilon} H_n \cdot \psi_n \cdot \cos(n\pi(\eta + \varepsilon)) \sin(n\pi\varepsilon) \right\}, \tag{31}$$

respectively, where

$$\gamma = \alpha + \frac{1}{2Bi\beta}, \tag{32}$$

$\varphi_n, \chi_n, \psi_n$ and σ_n are parameters defined by Lee and Leong (2013).

7. Position of the Auxiliary Heaters

To determine an adequate position f (or δ) of the auxiliary heater within the "exterior" portion along $\zeta = 0$ (or $y = 0$), Equations (29) to (31) will be used to determine the effect of position f (or δ) on R^*_{ht-c} (Equation (19b)). Also, with a proper choice of f, it is desired that the temperature non-uniformity along the bottom-interior portion of the plate, δT, be less than 1% of the overall temperature difference ($\Delta T = T_h - T_c$). The choice f (or δ) within the constraints of the physical space may not be optimal, but as long as $|\delta T / \Delta T| \leq 0.01$, the requirement of the "uniform" temperature profile along the bottom-interior portion of the plate has been met.

Figure 6 shows the dependence of R^*_{ht-c} as a function of $-q^*$, t (auxiliary heat flux profile), and δ (position of the auxiliary heater). Two particular sets of values for δ have been chosen for plotting R^*_{ht-c} with $-q^*$: $\delta = 0$ and $2\rho = 0.0641$ ($f = 0$ and $2g = 5$ mm), and $\delta = 2\rho = 0.0641$ ($f = 2g = 5$ mm). Figure 6 shows that for each δ, R^*_{ht-c} is also insensitive to t (for $t = -\frac{1}{2}, 0, \frac{1}{2}$), which coincides with the observations reported by Lee and Leong (2013) and Schneider et al. (1980). Therefore, the uniform heat flux profile, i.e. $t = 0$, is a good approximation, which will be used in the subsequent analyses.
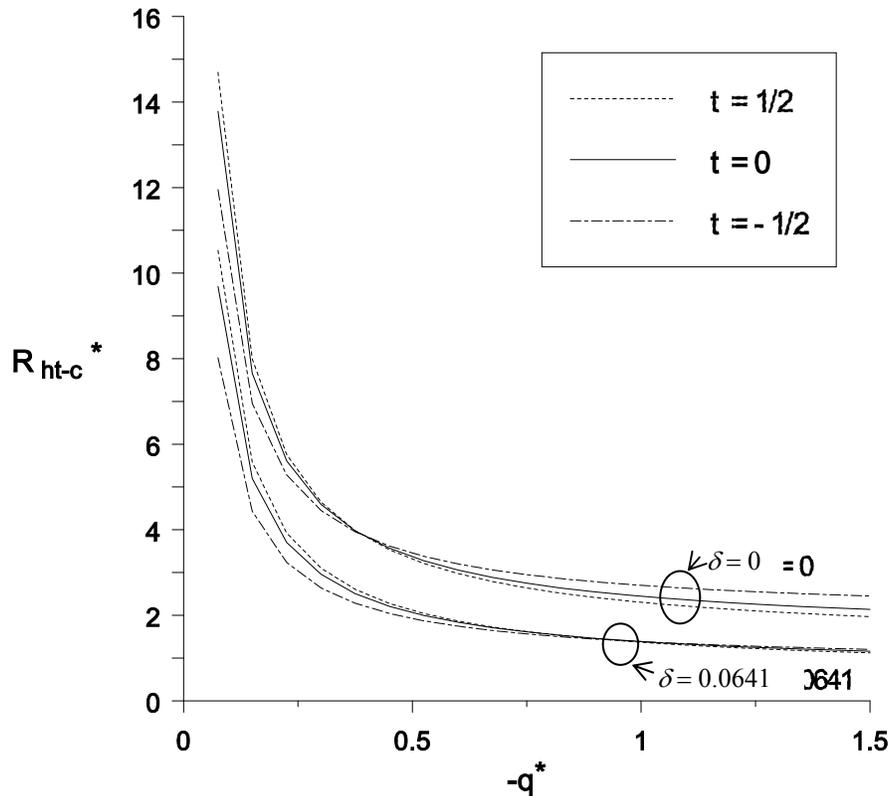

Figure 6. The effect of thermal resistance between the auxiliary heater and the sidewall with $-q^*$

A qualitative assessment is made based on the sensitivity of R^*_{ht-c} with respect to $-q^*$ from Figure 6. It can be seen that for $-q^*$ greater than 1.0, R^*_{ht-c} is relatively small compared to values of R^*_{ht-c} when $-q^*$ is much less than 1.0. Other qualitative assessments can be made from Figure 6:

1. The choice of the auxiliary heater heat flux profile t does not strongly affect R^*_{ht-c};
2. The auxiliary heater should be placed as close to the sidewall as possible (that is, $f = 2g = 5$ mm or $\delta = 2\rho = 0.0641$); and

C. Lee and Leong: Temperature Boundary Condition on a Wall of an Enclosure: Part II

AAM: Intern. J., Vol. 8, Issue 1 (June 2013)   69

3. The choice of $-q^*$ should be greater than approximately 1.0 in order to reduce R^*_{ht-c} to a significant level (as shown in Figure 6).

Also, to determine the position f of the auxiliary heater, two requirements need to be met so that a "uniform" temperature condition can be met:

1. Along the bottom-interior portion of the "hot" plate, (i.e., $0.182 \leq \xi \leq 1$ and $\zeta = 0$, see Figure 3a), $\delta T'/\Delta T$ must be less than ±1%, where $\delta T'$ is the temperature *deviation* defined by

$$\delta T' = T_{\max} - \overline{T},$$ (33)

where T_{max} and $\overline{T}$ are the maximum and average temperatures along the bottom-interior portion of the "hot" plate, respectively.

2. The temperature difference

$$\delta T = T(\xi_2, 0) - T(\xi_1, 0)$$ (34)

is minimized between the two locations within the "hot" plate ($\xi_1 = 0.162$ and $\xi_2 = 0.75$) along the bottom-interior of the plate ($\zeta = 0$), such that $\delta T/\Delta T$ is also less than ±1%. The temperature difference between these two points was measured by a pair of thermocouple junctions in thermopile arrangement embedded in the plate (Leong (1996)).

In achieving these two requirements, it is envisioned that the first requirement would also be satisfied when δT is minimized.

Since the contact length of the auxiliary heater, $2g$, needs to be positioned, a convenient choice $f = 2g$ is made. The results for a particular value of $\delta = 2\rho = 0.0641$ (that is, $f = 2g = 5$ mm) are tabulated in Table 2 for the four ΔT (= $T_h - T_c$) cases (Cases #1 through #4, Leong (1996)). The results based on the analysis demonstrate that by placing the auxiliary heater at $\delta = 0.0641$ with contact length $2\rho = 0.0641$, the temperature non-uniformity $\delta T/\Delta T$ along the bottom-interior of the plate is within ±1% when $-q^*$ is chosen to be approximately 1.4. At these specifications, about 80% of heat emanating from the auxiliary heater transfers to the sidewall (based on Equation (22)). The remainder of heat from the auxiliary heater transfers to the circulating fluid located at the opposite side of the "hot" plate. It is important to note here that there may be other combinations of δ, ρ and $-q^*$ which may equally provide the desired temperature non-uniformity $\delta T/\Delta T$ of less than ±1%. Also shown in Table 2 is a comparison of $\delta T/\Delta T$ based on the current analysis using the approximate analytical solution and the measured data (Leong (1996)) for Case #2. There is very good agreement between these two sets of results.

Table 2. Summary of results by minimizing δT for $\delta = 2\rho = 0.0641$
[†]measured Data (Leong (1996))

Case #	ΔT (K)	$-q^*$	Q_{ht-c}/Q_{ht}	$\delta T/\Delta T$	$\delta T'/\Delta T$
1	4.08	1.395	81.7%	-0.03%	0.28%
2	11.9	1.410	80.8%	-0.03%	0.28%
		1.44[†]		0.041%[†]	
3	21.2	1.439	79.1%	-0.03%	0.28%
4	31.2	1.441	79.1%	-0.03%	0.28%

A comparison of the relative temperature distributions, $T(x, 0) - T(0.078, 0)$ along $y = 0$ between the approximate analytical temperature solution, given by Equation (29), with the Finite-Element Method (FEM) solution is obtained for Case #4 and plotted in Figure 7. As noted in the Figure 7, there is excellent agreement of the relative temperature solutions based on the present approximate analytical temperature solution with the FEM temperature solution.
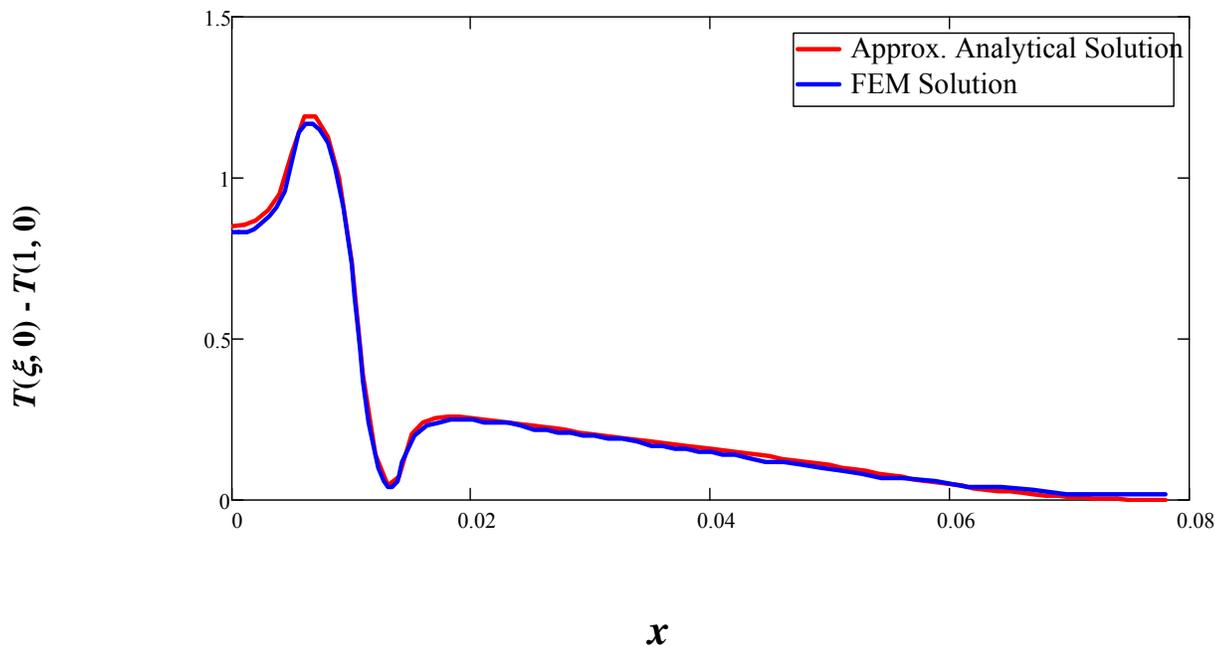

Figure 7.   Comparison of the relative temperature Distributions, $T(X, 0) - T(0.078, 0)$, along $Y = 0$ for case #4 With $\varDelta = 2\rho = 0.0641$ (or $F = 2g = 5$ Mm) based on the approximate analytical solution and the Fem solution

Now, to demonstrate the effectiveness of the auxiliary heater, dimensionless relative temperature distributions $T^*(\xi, 0) - T^*(1, 0)$ along $\zeta = 0$ (or $y = 0$) for Case #4 is plotted in Figure 8 with and without the auxiliary heater. Although there may be other chosen values of f, $2g$, and $-q^*$, it is

C. Lee and Leong: Temperature Boundary Condition on a Wall of an Enclosure: Part II

AAM: Intern. J., Vol. 8, Issue 1 (June 2013)   71

clear that by adding the auxiliary heater and by choosing $\delta = 2\rho = 0.0641$ (or $f = 2g = 5$ mm), temperature non-uniformity is significantly reduced to within 1% for $0.182 \leq \xi \leq 1$.
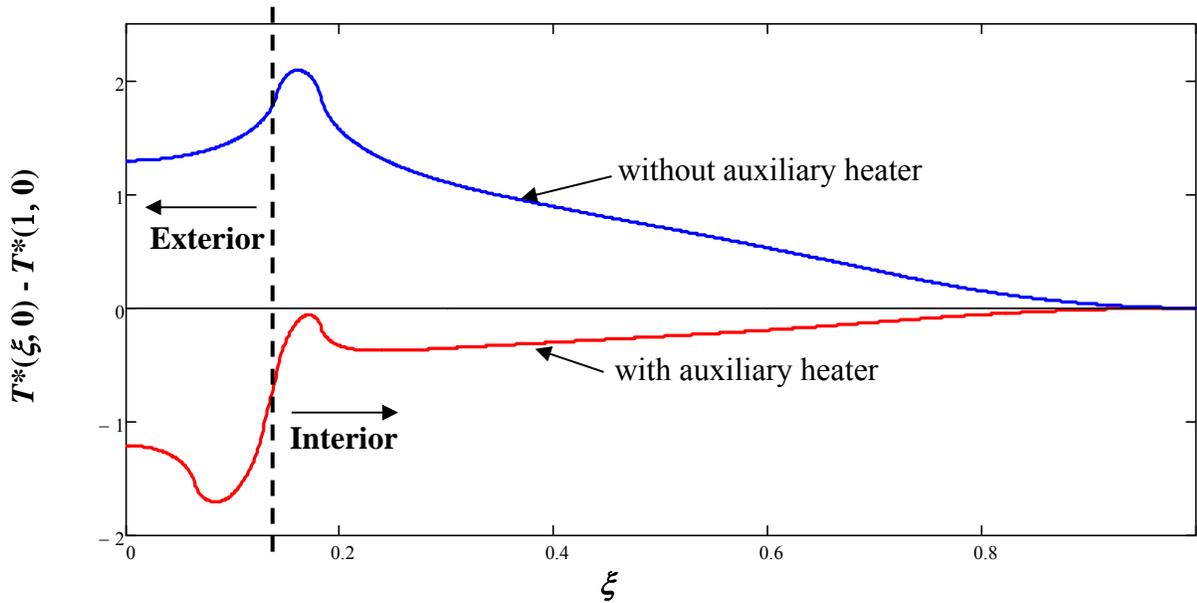

Figure 8. Dimensionless relative temperature distributions, $T^*(\Xi, 0) - T^*(1, 0)$, along $Z = 0$ for case # 4 with $\Delta = 2\rho = 0.0641$

To assess whether the effect of thermal spreading/constriction resistance $R^*_{s/c}$ between the contact region and the circulating fluid has been reduced by the addition of the auxiliary heater, Figure 9 illustrates the dependence of $R^*_{s/c}$ on $-q^*$. Thermal spreading/constriction resistance $R^*_{s/c}$ is defined as the difference between the *overall* thermal resistance $R^*_{c,f}$ (Equation (31)) and γ, the sum of the thermal resistances due to conduction and convection at solid-fluid boundaries (Equation (32)), which is given by

$$R^*_{s/c} = R^*_{c,f} - \gamma . \tag{35}$$

As shown in Figure 9, the effect of $R^*_{s/c}$ is reduced from 1.2 to zero as $-q^*$ increases from 0 to 0.67, respectively, and $R^*_{s/c}$ further decreases linearly as a negative value for $-q^* > 0.67$. This can be explained by examining the definition of $R^*_{c,f}$ (Equation (16)): the mean temperature at the contact region exceeds that of the mean circulating-fluid temperature for $-q^* > 0.67$, which causes $R^*_{s/c}$ to increase negatively (since $Q < 0$). Physically, for $-q^* > 0.67$, there has been an increase of heat flow from the auxiliary heater to the circulating fluid $Q_{ht\text{-}f}$.
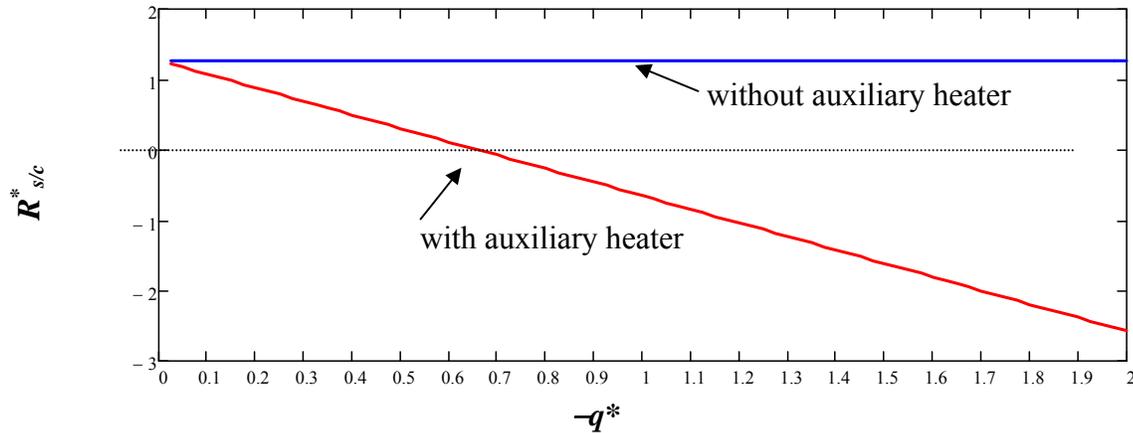
Figure 9. The Variation of Thermal Spreading/Constriction Resistance, $R^*_{s/c}$, with $-q^*$

8.   Concluding Remarks

Wall temperature non-uniformity on a "hot" plate of a three-dimensional experimental apparatus was reduced from approximately 4% to less than 1% of the overall temperature difference. This was achieved by placing auxiliary heaters on the "exterior" portions of the "hot" main plate. A mathematical model was developed and an approximate analytical temperature solution was presented. A detailed analysis was conducted by using this approximate temperature solution to examine the effect of the position of the auxiliary heater on the exterior portion of the "hot" main plate. Temperature difference between two points on the bottom-interior portion of the hot plate shows a reduction of temperature non-uniformity to an acceptable level to render the "uniform" temperature condition physically-realizable. Thermal resistance analyses show that the temperature non-uniformity can be reduced to within 1% by placing the auxiliary heaters close to the sidewall. Based on the present mathematical analysis, the original design was successfully modified to conduct the benchmark internal natural convection experiment originally intended.

Also, the approximate analytical temperature solution can serve to validate any computer codes for simulating heat conduction problems, and can be adapted to analyze a number of similar engineering applications: for example, but are not limited to, in design analyses of solar collector plates; in radioactive cooling of panels on satellites and/or spacecraft's; and in thermal management of micro-electronic circuits.

Acknowledgements

C. Lee and Leong: Temperature Boundary Condition on a Wall of an Enclosure: Part II

AAM: Intern. J., Vol. 8, Issue 1 (June 2013) 73

Nomenclature

a	= half-width of contact at sidewall, m
Bi	= Biot number/modulus, hb/k, or R_{cond}/R_{conv}
b	= width of plate, m
c	= plate thickness, m
d	= fluid contact width, m
e	= location of the sidewall, m
f	= location of the auxiliary heater, m
$F_n(\eta,\varepsilon)$	= functional form for sidewall heat flux profile
$G_n(\delta,\rho)$	= functional form for auxiliary heater heat flux profile
g	= half width of contact of auxiliary heater, m
h	= heat transfer coefficient, W/(m^{2}K)
k	= thermal conductivity, W/(mK)
L	= length of plate into the page, m
m, t	= shape parameter for heat flux profile, $q(x)$ and $q_1(x)$, respectively
Q	= total heat flow at sidewall, Equation (5), W
$q(x)$	= heat flux profile of the sidewall, W/m^2
$q_1(x)$	= heat flux profile of the auxiliary heater, W/m^2
R	= thermal resistance, K/W
$R_{c,f}$	= sidewall (contact) to fluid thermal resistance based on Q, K/W
$R_{c\text{-}f}$	= sidewall (contact) to fluid thermal resistance based on $Q_{c\text{-}f}$, K/W
$R_{ht\text{-}c}$	= auxiliary heater to sidewall (contact) thermal resistance based on $Q_{ht\text{-}c}$, K/W
R_o	= overall/total thermal resistance, K/W
$R_{s/c}$	= spreading/constriction thermal resistance, K/W
T	= temperature, K
$\bar{T}$	= mean temperature, K
u, v	= local co-ordinates for the sidewall and auxiliary heater heat flux distributions
x, y	= Cartesian co-ordinate system
α	= dimensionless thickness, c/b
β	= dimensionless fluid contact width, d/b
$\chi_n, \varphi_n, \psi_n$	= function/parameter
δ	= dimensionless position of the auxiliary heater, f/b
δT	= temperature difference, $T(\xi_2, 0) - T(\xi_1, 0)$, K
$\delta T'$	= temperature deviation, difference between maximum and mean temperatures, K
ε	= dimensionless half contact length, a/b
γ	= dimensionless conduction and convection resistances
η	= dimensionless distance to sidewall location, e/b
ρ	= dimensionless half contact length, g/b
$\sigma_n, \sigma_{i,n}$	= function/parameter
ξ, ζ	= dimensionless co-ordinate, x/b and y/b

Superscripts
*	= dimensionless variable

Subscripts
1, 2	= subsection of circulating fluid

c   = sidewall (or contact), or otherwise noted
f   = fluid
ht   = auxiliary heater

REFERENCES

de Vahl Davis, G. (1983). Natural Convection of Air in a Square Cavity: A Benchmark Numerical Solution, Int. J. Numerical Methods Fluids, **3**, pp. 249 – 264.

de Vahl Davis, G. and Jones, I.P. (1983). Natural Convection in a Square Cavity: a Comparison Exercise, Int. J. Numerical Methods Fluids, **3**, pp. 227-248.

El Sherbiny, S.M., Hollands, K.G.T., and Raithby, G.D. (1982). Effect of Thermal Boundary Conditions on Natural Convection in Vertical and Inclined Air Layers, J. of Heat Transfer, **104**, pp. 515 – 520.

Gradshteyn, I.S. and Ryzhik, I.M. (1965). *Tables of Integrals, Series, and Products*, 4th Ed., Academic Press, New York.

He, S. and Gotts, J.A. (2005). A Computational Study of the Effect of Distortions of the Moderator Cooling Channel of the Advanced Gas-Cooled Reactor, Nuclear Engineering and Design, **235**(9), pp. 965-982.

Le Quere, P. (1991). Accurate Solutions to the Square Thermally Driven Cavity at High Rayleigh Number, Computers Fluids, **20** (1), pp. 29 – 41.

Lee, P.Y.C. and Collins, W.M. (1998). Moderator Circulation Analysis for the Modified CANDU 6 Design using the CFD Code MODTURC_CLAS, Proceedings, 19th Annual Canadian Nuclear Society Conference, Toronto, Ontario, Canada, **2**, Session 5C – Safety, pp. 1 – 9.

Lee, P.Y.C. and Leong, W.H. (2013). Physically-Realizable Uniform Temperature Boundary Condition Specification on a Wall of an Enclosure: Part I – Problem Investigation, International Journal of Applications and Applied Mathematics (AAM).

Leong, W.H. (1996). Benchmark Experiments on Natural Convection Heat Transfer Across a Cubical Cavity, Ph.D. Thesis, Department of Mechanical Engineering, University of Waterloo, Waterloo, Ontario, Canada.

Leong, W.H., Hollands, K.G.T. and Brunger, A.P. (1998). On a Physically-Realizable Benchmark Problem in Internal Natural Convection, Int. J. Heat Mass Transfer, **41** (23), pp. 3817-3828.

Leong, W.H., Hollands, K.G.T. and Brunger, A.P. (1999). Experimental Nusselt Numbers for a Cubical-Cavity Benchmark Problem in Natural Convection, Int. J. Heat Mass Transfer, **42** (11), pp. 1979-1989.

Schneider, G.E., Yovanovich, M.M. and Cane, R.L.D. (1980). Thermal Resistance of a Convectively Cooled Plate with Nonuniform Applied Flux, J. Spacecraft Rockets, AIAA 78-86R, **17** (4), pp. 372-376.